ACS APPLIED MATERIALS & INTERFACES

Research Article

www.acsami.org

Hierarchical Polymer Brush Nanoarrays: A Versatile Way to Prepare Multiscale Patterns of Proteins

Yunfeng Li,[†] Junhu Zhang,[†] Wendong Liu,[†] Daowei Li,[‡] Liping Fang,[†] Hongchen Sun,[‡] and Bai Yang*[,†]

[†]State Key Laboratory of Supramolecular Structure and Materials, College of Chemistry, [‡]School of Stomatology, Jilin University, Changchun 130012, P. R. China

Supporting Information

ABSTRACT: This paper presents a versatile way to prepare multiscale and gradient patterns of proteins. The protein patterns are fabricated by conjugating proteins covalently on patterns of polymer brush that are prepared by techniques combining colloidal lithography with photolithography, and two-step colloidal lithography. Taking advantages of this technique, the parameters of protein patterns, such as height, diameters, periods, and distances between two dots, can be arbitrarily tuned. In addition, the protein patterns with varies of architectures, such as microdiscs, microstripes, microrings, microtriangles, microgrids, etc., consisting of protein nanodots, are prepared and the sample size is up to 4 cm^2. The as-prepared patterns of fibronectin can promote the cell adhesion and cell location.

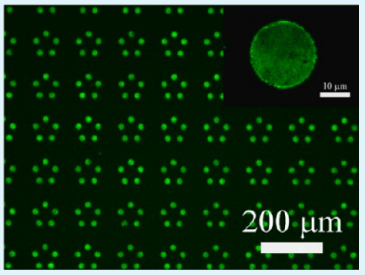

KEYWORDS: *protein patterns, colloidal lithography, polymer brush, cell adhesion, multiscale*

1. INTRODUCTION

Patterning proteins and other biomolecules at the nanoscale is of great importance for medical and biological applications, including biosensors, drug screening, and research of cell biology.[1−7] For example, protein and DNA nanopatterns can be used to detect the proteome and genome content in a highly parallel fashion, which has resulted in improved medical diagnostic technologies.[4] Nanopatterns possess advantages compared to microarrays, including the higher density of reaction sites and much smaller sample volume, so they can lead to potentially higher sensitivity and improved kinetics.[5] In addition, nanostructured surfaces play an important role in research related to living cells.[6,7]

Living cells are exquisitely sensitive to the hierarchical adhesive extracellular matrix (ECM) microenvironment.[6] The ECM typically consists of a viscoelastic network of nanofibrous proteins, such as collagen molecules which are approximately 300 nm long and 1.5 nm wide, and these molecules form fibrils that extend for tens of micrometers in length.[6] An immense amount of research efforts have focused on understanding the fundamental mechanism of interactions between cells and artificially nanostructured surfaces via protein patterning and how these surfaces relate to the subsequent cellular response.[8] Protein nanopatterns with controllable features are a theme of biomimetics that aims to recapitulate an in vivo-like environment in order to precisely manipulate the behavior of living cells and interpret the signaling mechanism of interaction between the cells and matrix.[7] The engineering of protein nanoarrays can pave a novel way to induce desired cell phenotypes and genotypes, and to study the principle of stem-cell differentiation.[6] Besides these research goals, the protein nanopattens can help to optimize the architectures of biomaterials, including morphology, surface nano-topography and bioactivity, which shows a strong potential for significant improvement of tissue engineering and wound healing.[9]

The past decade has witnessed the rapid development of the preparation of protein nanopatterns.[1] Despite these efforts, with respect to achieving broad applications, a major challenge is still in developing an effective way to prepare multiscale and gradient type patterns of bioactive proteins surrounded by a stable protein adsorption-resistant background. In general, two approaches can be used to prepare protein patterns, namely patterning by absorption and patterning by covalent bond. For the former approach, protein patterns are fabricated by making use of forces of physical absorption between proteins and substrate by relying on micro- or nanofabrication techniques, such as microcontact print, scanning probe microscopy lithography and methods based on colloidal science.[10−19] For the latter approach, protein patterns are prepared through covalently immobilizing proteins on a reactive or patterned layer.[20−25] Such layers are usually made of reactive self-assembled monolayers or polymer layers.[26,27] Recently, polymer brushes have been used to immobilize proteins covalently. These proteins exhibit three-dimensional (3D) distributions on the polymer brush while maintaining efficiently their biological activity.[28,29] Several methods have been used to prepare patterns of polymer brush, such as nanoimprint lithography, electron beam lithography, electro-oxidative lithography, Langmuir−Blodgett lithography, etc.[30−40] Few reports of protein patterns exist, however, based on the fabricated patterns of polymer brush.[41]

Received: December 19, 2012
Accepted: February 21, 2013
Published: February 21, 2013

In this paper, we report a novel method to fabricate multiscale and gradient patterns of proteins by covalently immobilized proteins on the hierarchical poly(2-hydroxyethyl methacrylate) (PHEMA) brush patterns. The hierarchical PHEMA brush nanopatterns are fabricated by method that combines colloidal lithography with photolithography, and two-step colloidal lithography. By using colloidal lithography,[42−45] the parameters of polymer nanopatterns, such as height, diameters, periods, and distances between two polymer dots, can be arbitrarily tuned. Different types of multiscale polymer brush patterns, such as microdiscs, microstripes, microrings, microtriangles and microgrids etc., consisting of polymer brush nanodots, are fabricated by photolithography and oxygen plasma etching. In addition, multiscale and gradient polymer brush patterns are prepared by two-step colloidal lithography. More importantly, various multiscale and gradient protein patterns are fabricated after covalent immobilization of proteins on the polymer brush, and these proteins maintain good biological activity. As a proof-of-concept work, as-prepared fibronectin (FN) patterns are used to fabricate cell patterns.

2. EXPERIMENTAL METHODS

Materials. Silicon wafers (100) and fused silica wafers were cut in ca. 2.0 × 2.0 cm^2 pieces. HEMA monomer, 2, 2′-bipyridine, phosphate buffer saline and $CuBr_2$ were provided by Alfa. Aminopropyltrimethoxysilane (ATMS), 2-bromoisobutyryl bromide, 4-dimethylaminopyridine (DMAP), N, N′-disuccinimidyl carbonate (DSC), CuCl, tetramethylrhodamine B isothiocyanate (TRITC) labeled phallaoidin, 4,6-diamidina-2-phenylindole (DAPI), albumin bovine serum, and anti-vinculin were purchased from Aldrich. Poly(ethylene glycol)-silane (PEG-silane) (M_w = 1000) was provided by Shanghai Yare Biotech. Fibronectin (FN) was provided by Shanghai EYSIN Biotechnology. 4% polyoxymethylene, Triton-X100, human immunoglobulin G (IgG) and FITC-labeled goat anti-human IgG were purchased from Beijing DINGGUO Biotechnology. Dichloromethane, toluene, triethylamine, and absolute ethanol were used as received. The water used in all experiments was deionized and doubly distilled prior to use.

Grafting PHEMA from Surfaces. The detailed method to prepare PHEMA brush on the silicon and fused silica wafers has been given in our previous work.[46] In brief, the silicon wafers and fused silica wafers were cleaned in the mixture of 98% H_2SO_4/30% H_2O_2 (volumetric ratio 7:3) for 30 min under boiling (Caution: strong oxide), and then rinsed with deionized water and absolute ethanol several times, and lastly dried with an N_2 stream. Next, these wafers were placed in a sealed vessel, on the bottom of which was a few drops of ATMS. The vessel was put in an oven at 60 °C for 1 h to enable the ATMS vapor to react with the −OH groups on the silicon or silica wafers. After that, wafers functionalized with -NH_2 were immersed in the solution of 10 mL anhydrous dichloromethane with 100 μL triethylamine. The atom-transfer radical polymerization (ATRP) initiator, 2-bromoisobutyryl bromide, was added dropwise into the solution at 0 °C, and the mixture was left for 1 h at this temperature then at room temperature for ca. 15 h. The wafers were cleaned by anhydrous dichloromethane three times and absolute ethanol three times, and dried by N_2 flow.

For polymerization of PHEMA, 36 mg (0.16 mmol) of $CuBr_2$ and 244 mg of 2,2′-bipyridine (1.56 mmol) were added to 8 mL of an aqueous solution of monomer (HEMA/H_2O, 1:1 V:V), and the mixtures were shaken in a ultrasonic bath until a homogeneous blue solution formed. The mixtures were degassed by 30 min ultrapure nitrogen flow, 55 mg (0.55 mmol) CuCl was added into the solution, and it was shaken in a ultrasonic bath and changed into dark brown. Lastly the wafers with initiators were immersed in the solution from 1 to 12 h under the nitrogen flow at room temperature. After polymerization, the samples were cleaned by absolute ethanol and deionized water by washing several times.

Patterning of PHEMA Brush. PHEMA brush nanopatterns were prepared by colloidal lithography using a 2D polystyrene (PS) colloidal crystal as a mask. First, 2D PS colloidal crystals were prepared by a modified interfacial method on the wafers with PHEMA brush films. The PS microspheres used in our work were 320 nm and 580 nm. Subsequently, oxygen reactive ion etching (RIE) operating at 10 mTorr pressure, 50 SCCM flow rate, and RF power of 30 W with an ICP power of 100 W was carried out for a length of time ranging from 90 to 420 s. Finally, PHEMA brush nanopatterns were obtained after the remaining PS microspheres were removed by chloroform under an ultrasonic bath.

The multiscale patterns of the PHEMA brush were prepared by combining colloidal lithography with photolithography. A positive photoresist was spin-coated on a cleaned wafer with PHEMA brush nanopatterns and patterned by conventional photolithography techniques using a mask. Subsequently, the PHEMA brush on the wafer without covering of photoresist was removed by O_2 plasma. Hierarchical patterns of polymer brush were obtained after the wafers were finally rinsed with acetone and absolute ethanol to remove the photoresist and dried with N_2 flow.

The multiscale, gradient patterns of the PHEMA brush were prepared by two-step colloidal lithography. A PS colloidal crystal with a period of 3.7 μm was prepared by interfacial method on the wafers with PHEMA brush nanopatterns. Subsequently, oxygen RIE was performed using the same conditions mentioned for 8 min. After that, the complex patterns of polymer brush were achieved after removing the remaining PS microshperes.

Preparing the Multiscale Patterns of Proteins. To reduce nonspecific absorption of proteins on the background, we immersed the freshly prepared nanopatterns of polymer brush in a solution of PEG-silane in anhydrous toluene for 12 h at room temperature. The wafers were then rinsed by toluene and absolute ethanol several times, and dried using an N_2 flow. The samples were immersed in a deoxygenated solution of 0.1 M DSC and DMAP in anhydrous dimethylformamide (DMF) for 24 h. The samples were rinsed thoroughly with DMF and dichloromethane, and then dried by an N_2 flow. When conjugating proteins to the polymer brush, the modified samples were immersed in a solution of human IgG (50 μg/mL) or fibronectin (FN) (50 μg/mL) in PBS for 2 h at room temperature. After that, the wafers were rinsed by PBS several times to remove the absorbed proteins on the surfaces of samples. To evaluate the activity of the human IgG, we immersed the wafers with human IgG patterns in a solution of FITC-labeled goat anti-human IgG (50 μg/mL) in PBS for 1.5 h. The wafers were rinsed using PBS several times to remove the nonspecifically absorbed proteins.

Cell Seeding and Staining. Mouse MC3T3-E1 osteoblasts were plated at a density of 1×10^5 cells per mL in H-DMEM media supplemented with 10% fetal bovine serum (FBS) (Gibco) and 1% antibiotics (25.000 IU/mL penicillin and 25 mg/mL streptomycin) in 5% CO_2 at 37 °C. After culturing for 3 h, cells on the substrates were washed in PBS, and incubated for approximately 1 min with fluorescein diacetate (FDA) stock (5 mg dissolved in 1 mL acetone) dissolved in PBS (10 μL/10 mL), and washed once more. For cell immunostaining, the cells were fixed by 4% polyoxymethylene in PBS solution for 20 min and permeabilized for 10 min with 0.1% Triton X-100. The cells were then incubated for 30 min at room temperature with a 3% bovine serum albumin blocking agent and washed twice with PBS buffer. Mouse monoclonal anti-vinculin 1.25 μg/mL was added to the cells and incubated for 3 h at 37 °C and washed three times in PBS. FITC-conjugated goat anti-mouse IgG (10 μg/mL) and TRITC-phalloidin (100 ng/mL) were added to the surfaces and incubated for 60 min at room temperature. Cells were thereafter washed three times with PBS and finally incubated for 5 min at room temperature with 2 μg/mL DAPI and washed three times. Stained cells were kept in PBS at 4 °C.

Characterization. The atomic force microscopy (AFM) images were recorded in tapping mode with a Nanoscope IIIa scanning probe microscope from Digital Instruments under ambient conditions. SEM micrographs were taken with a JEOL FESEM 6700F electron microscope with primary electron energy of 3 kV. The samples were

sputtered with a thin layer of Pt prior to imaging. The photograph and fluorescent images of the samples were taken by OLYMPUS BX51. The thicknesses of the PHEMA brush films were measured by Dektak150 surface profiler (Veeco).

3. RESULTS AND DISCUSSIONS

3.1. Preparation of PHEMA Brush Nanopatterns by Colloidal Lithography. The nanopatterns of PHEMA brush are fabricated by oxygen reactive ion etching (RIE) films of PHEMA brush using two-dimensional (2D) polystyrene (PS) colloidal crystals as masks. The procedures of fabricating polymer brush patterns are described in detail in the experimental section. Briefly, a film of PHEMA brush is prepared by surface-initiated atom-transfer radical polymerization (SI-ATRP) from an initiator monolayer on a silicon or fused silica substrate (see Figure S1a in the Supporting Information).[46] Subsequently, a 2D PS colloidal crystal is prepared by the modified interface method on the substrate with a film of PHEMA brush (see Figure S2 in the Supporting Information).[47] Finally, PHEMA brush patterns are fabricated by oxygen RIE using 2D PS colloidal crystal as masks.[48] Films of PHEMA brush are high-quality and homogenous over a wafer area with an RMS below 1 nm (see Figure S1a in the Supporting Information). The thickness of the PHEMA brush can be precisely controlled by changing the duration of polymerization as a consequence of the nature of living polymerization (see Figure S1b in the Supporting Information). Figure S2 in the Supporting Information shows the 2D PS colloidal crystals used as masks for patterning the polymer brushes. The PS microspheres exhibit hexagonal packing on the substrate over a large area, which contributes to the formation of high-quality polymer brush nanopatterns.

Colloidal lithography, as a parallel technique of microfabrication, allows preparing patterns in high-fidelity, large area and low cost fashion, and can easily control the features of the as-prepared patterns.[42−45] Figure 1 presents the atomic force microscopy (AFM) images of PHEMA brush patterns by etching a 125 nm PHEMA film for 120 s (Figure 1a), 240 s (Figure 1b), 300 s (Figure 1c), and 360 s (Figure 1d) using a 2D PS colloidal crystal of 580 nm in period (see Figure S2a in the Supporting Information) as masks. As the duration of RIE etching increases, the diameter of the polymer brush nanodot decreases and the distance between the nanodots increases. The formation mechanism of PHEMA brush patterns can be explained as follows. In the process of colloidal lithography, the PS colloidal crystal is also etched by oxygen plasma. During the beginning stage, the PHEMA brush films are etched by oxygen plasma through voids among the PS microspheres. After etching 120 s, and then removing the PS microspheres, bridged polymer brush patterns are formed on the substrate that are ca. 114 nm in height, the tops of which are relatively smooth. In these cases, excess polymer brush exists between the nanodot of polymer brush as a result of the lack of platform in the cross-sectional profile of PHEMA brush patterns (Figure 1a). When the etching time increases to 240 s, the polymer brush and PS microspheres are etched substantially more, and the PHEMA brush patterns also exhibit bridged morphologies that are ca. 120 nm in height. Almost no polymer brush is left in the defect regions. The resulting morphology is more tapered than that of samples etched for 120 s (Figure 1b). After etching for 300 s and 360 s, the polymer brush patterns exhibit isolated morphologies which are ca. 77 nm and 65 nm in height. In these cases, the PS microshperes are etched completely, the

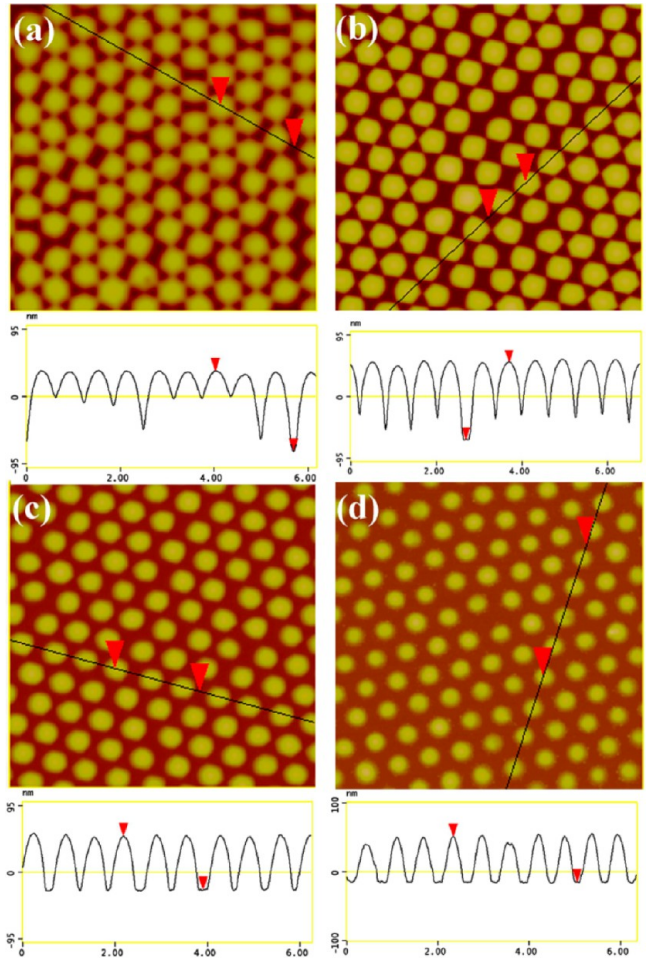

Figure 1. AFM images and cross-sectional profiles of PHEMA brush nanopatterns by etching PHEMA brush films of 125 nm for (a) 120, (b) 240, (c) 300, and (d) 360 s, sizes are 6 μm × 6 μm.

heights of polymer brush patterns will decrease and the distance between the polymer nanodots will increase due to the absence of the masks of microshperes. In this work, the polymer brush patterns exhibit tapered profile; however, such tapered profiles are not caused by the lateral spreading of the chains at the edge of the polymer brush nanodots.[33] The patterns of polymer brush are etched on the films of polymer brush, but are not grafted from the patterns of ATRP initiators. Therefore, the lateral resolution of polymer brush patterns is easier to control precisely.[49,50]

The patterns of PHEMA brush can be also tuned by changing the thickness of PHEMA brush films. For example, films of PHEMA brush in 65 and 170 nm thicknesses are etched by oxygen plasma for 180 s and 300 s respectively, and the 3D AFM images of the polymer brush patterns are shown in Figure S3 in the Supporting Information. We can see that their morphologies are almost the same and the heights of PHEMA brush patterns are ca. 50 nm (see Figure S3a in the Supporting Information) and 130 nm (see Figure S3b in the Supporting Information), respectively. In addition, patterns of polymer brush with different periods can be easily prepared by using PS colloidal crystals of different periods as masks in the process of colloidal lithography. Figure S4 in the Supporting Information presents the patterns of PHEMA brush that are 320 nm in period. The PHEMA brush nanodots exhibit

hexagonal non-close packing and are homogeneous over large areas.

The patterns of PHEMA brush prepared by this method possess some advantages. (1) By employing colloidal lithography, a polymer brush pattern with wafer scale can be prepared in a time-efficient and low-cost fashion, and the nanoarchitecture parameters of polymer brush patterns, such as period, height, and distance between polymer nanodots can be controlled arbitrarily. The chemistry of the polymer brush patterns can also be tuned by changing the kind of polymer brush films being used. (2) Preparation of patterns of polymer brush with precise lateral resolution is relatively simple because of the absence of lateral spreading of the chains at the edge of the polymer brush nanodots. (3) Colloidal lithography can be easily integrated with other techniques of microfabrication; therefore, many kinds of polymer brush patterns of multiscale, complexity, and gradient can be prepared rationally.

3.2. Multiscale and Gradient PHEMA Brush Patterns. The multiscale polymer patterns are crucial for self-cleaning surfaces, antifouling surfaces, biosensors and biological interfaces.[51,52] In this paper, multiscale PHEMA brush patterns are prepared by fabricating as-prepared PHEMA brush patterns using colloidal lithography making use of photolithography and oxygen plasma etching. The hierarchical PHEMA brush nanopatterns exhibit homogeneous architectures over wafer-scale and the borderlines between the regions with and without polymer brush nanodots are vivid. Figure 2a shows the

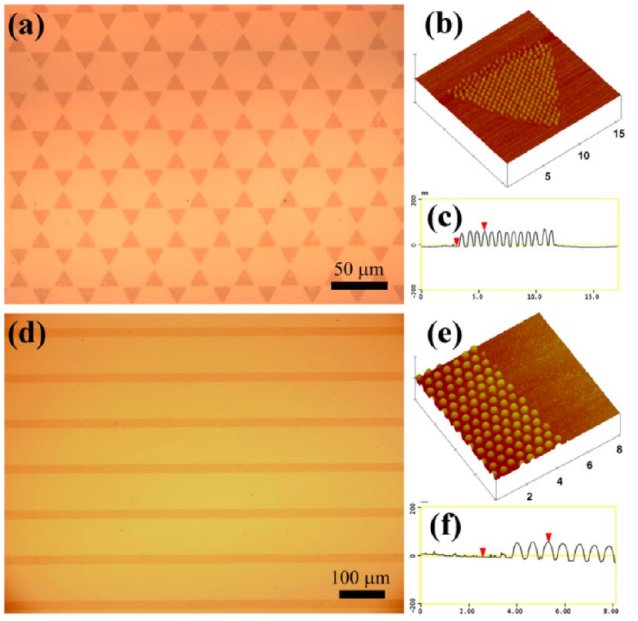

Figure 2. Photograph of the (a) microtriangle and (d) microstripes of the PHEMA brush patterns, the dark region is the polymer brush nanodots and the bright region is the substrate, (b, c) 3D AFM images and cross-sectional profiles of PHEMA brush microtriangle patterns, z scale is 400 nm, (e, f) 3D AFM images and cross-sectional profiles of PHEMA brush microstripe patterns, z scale is 400 nm.

microtriangle patterns on the silicon substrate, which are uniform over large areas. To address the detailed information of the hierarchical nanopatterns, we evaluated their morphologies by AFM. Figure 2b presents the 3D AFM image of a microtriangle. We can see that each microtriangle consists of PHEMA brush nanopatterns that are 580 nm in period and 68 nm in height (Figure 2c). By changing the masks in the process of photolithography, the types of the micropatterns can be arbitrarily changed. Figure 2d presents the microstripe patterns with and without PHEMA brush nanodots. The dark regions consist of PHEMA brush nanodots, and the light regions are the silicon substrate. We use AFM to evaluate the quality of microstripe patterns, which are shown in Figure 2e. The microstripes are made of PHEMA brush nanodots with a period of 580 nm and a height of 60 nm (Figure 2f).

Recently, multiscale, gradient polymer brushes have been found to have great potential in various applications such as microfluidic devices, sensors, and biophysical research.[30] In the present system, the gradient patterns of PHEMA brushes are fabricated by two-step colloidal lithography. Figure 3 shows the

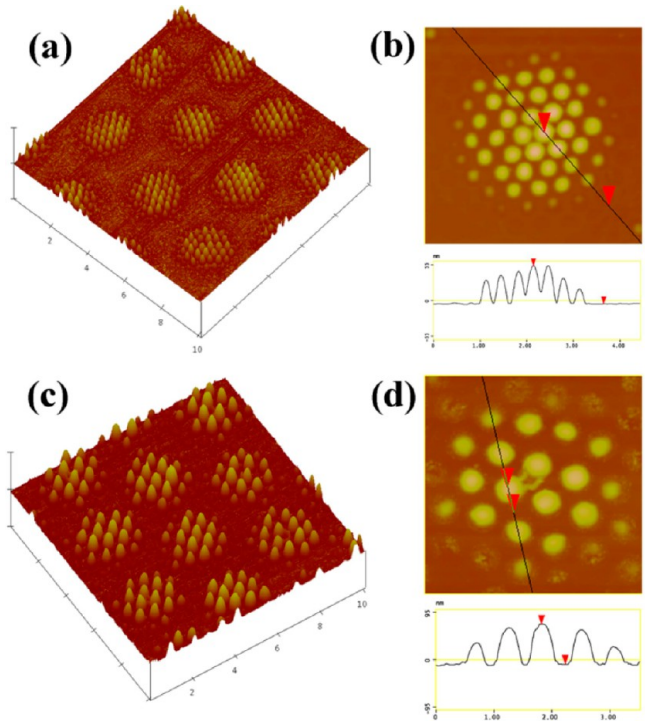

Figure 3. AFM images and cross-sectional profiles of multiscale and gradient patterns of PHEMA brush patterns. (a, b) 320 nm in period, z scale is 100 nm, (c, d) 580 nm in period, z scale is 200 nm.

3D AFM images of multiscale, gradient patterns of PHEMA brushes, and we can see that the patterns are homogenous. The microcircles exhibit hexagonal non-close-packed arrays, inheriting from the 2D PS colloidal crystals with a period of 3.7 μm. The microcircles consist of PHEMA brush nanodots with periods of 320 nm (Figure 3a) and 580 nm (Figure 3c), respectively. The heights and diameters of the PHEMA brush nanodots decrease from the centers to the edges of the nanodots (Figure 3b, d). The mechanism of formation of the gradient polymer brush patterns can be explained as follows. The multiscale and gradient polymer brush patterns are prepared by oxygen plasma etching, while the as-prepared nanopatterns of polymer brush are prepared through colloidal lithography using 2D PS colloidal crystals with a 3.7 μm period as masks. The distances between the microsphere and PHEMA brush nanopatterns gradiently enlarge from the center to the edge of microcircles as a consequence of the round profile of microsphere. The larger the space between the microspheres and substrate is, the higher the density of oxygen plasma scattering becomes. As a result, in the process of etching, the

dx.doi.org/10.1021/am3031757 | ACS Appl. Mater. Interfaces 2013, 5, 2126−2132

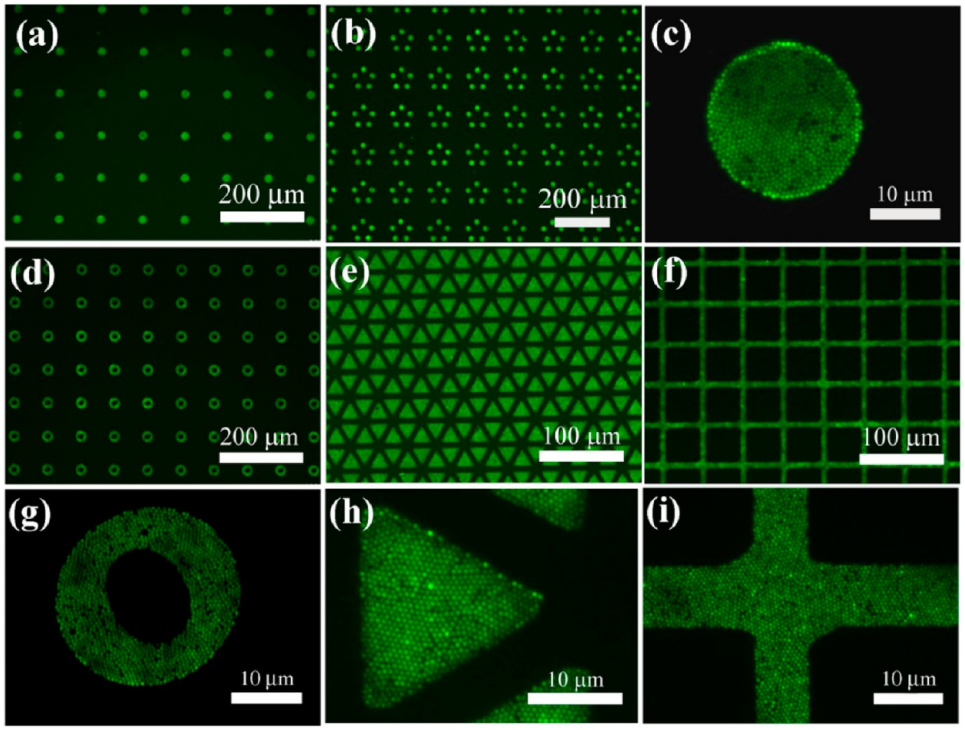

Figure 4. Fluorescent photograph of the multiscale IgG patterns after covalently bonding FITC-anti-IgG. (a–c) Microdisc protein patterns, (d, g) microring protein patterns, (e, h) microtriangle protein patterns, (f, i) microgrid protein patterns.

density of oxygen plasma gradiently increases from the centers to the edges of microcircles. Also the speed of etching in the regions below the microspheres gradiently increases from the centers to the edges of the microcircles. After removing what is left of the microspheres, the multiscale and gradient patterns of PHEMA brush are achieved. The feature sizes and chemical compositions of the polymer brush nanopatterns can be easily controlled by colloidal lithography, and the types of masks for photolithography can be designed arbitrarily, so the library of the multiscale and gradient polymer brush patterns can be constructed rationally. These multiscale and gradient patterns of PHEMA brushes will pave a novel way to fabricate complex, multiscale and gradient proteins and other biomacromolecules for practical applications.

3.3. Multiscale Patterns of Proteins. Multiscale protein patterns are fabricated by covalently immobilizing proteins on the PHEMA brush patterns. In order to reduce the absorption of proteins on the substrate, a monolayer of poly(ethylene glycol)-silane (PEG-silane) is immobilized on the regions without PHEMA brush patterns before conjugating with proteins. After that, patterns of PHEMA brush are immersed in a solution of 0.1 M N, N′-disuccinimidyl carbonate (DSC) and 4-dimethylaminopyridine (DMAP) in anhydrous dimethylformamide (DMF) to obtain the succinimidyl group modified PHEMA brush patterns. After modification by succinimidyl groups, the heights of PHEMA brush nanodots increase from ca 38 nm to 44 nm due to replacement of the small hydroxyl group by the larger succinimidyl group (see Figure S5a in the Supporting Information). Protein patterns can be easily fabricated by immersing a succinimide modified PHEMA brush nanopattens in a solution of human immunoglobulin G (IgG), because succinimidyl group are highly reactive with the primary amine groups of proteins. The PHEMA brush patterns used to prepare protein patterns are ca. 580 nm in period and 38 nm in height (see Figure S5a in the Supporting Information). The morphology of the IgG patterns undergoes almost no change (see Figure S5b in the Supporting Information), and the height of the protein patterns increases to about 62 nm after covalently immobilizing IgG (see Figure S5a in the Supporting Information).

To evaluate the biological activity of IgG, patterns of human IgG are immersed in a solution of FITC-labeled goat anti-human IgG in PBS, rinsed using PBS several times to remove the non-specifically absorbed proteins, and then the samples are investigated by fluorescence microscopy under blue light excitation (Figure 4). The IgG patterns are observed to be homogeneous over large areas and the signal intensity across the entire area is nearly the same throughout. These results indicate that the proteins are not denatured during the immobilization process. Many multiscale patterns of proteins can be prepared using the hierarchical patterns of the PHEMA brush as templates. As a proof-of-concept experiment, microdisc patterns (Figure 4a), five-microdisc patterns (Figure 4b), microring patterns (Figure 4d), microtriangle patterns (Figure 4e), and microgrid patterns (Figure 4f) have been fabricated and the proteins maintain their biological activity. After enlarging the micropatterns of proteins, we can see that each unit consists of nanodots that are 580 nm in period and every protein dot can be seen clearly (Figure 4c, g, h, i). The gradient patterns of proteins have been prepared by covalently immobilizing proteins on the gradient patterns of the PHEMA brush, which are shown in Figure S6 in the Supporting Information. We can see that the protein patterns exhibit hexagonal non-close-packed over wafer-scales, and the proteins maintain their activity. Moreover, preparation of the gradient protein patterns over a large area using conventional methods is by comparison a difficult task.

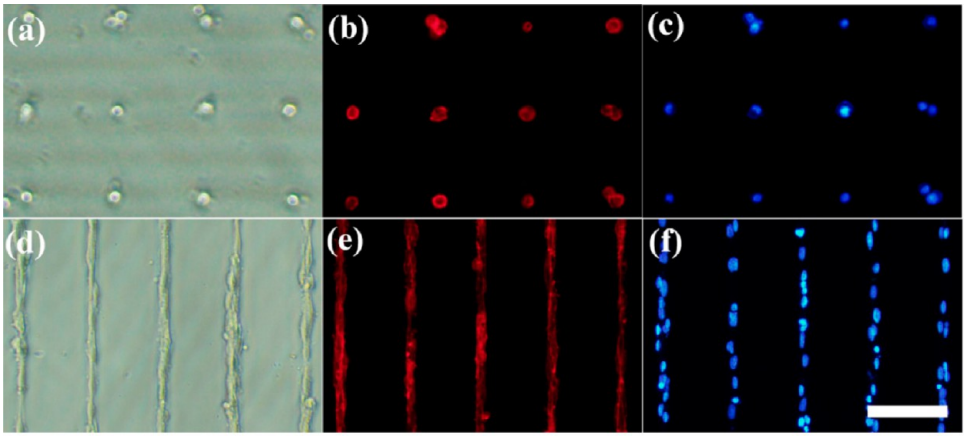

Figure 5. Cell adhesion on the FN patterns. (a, d) Phase contrast micrographs of mouse MC3T3-E1 osteblasts after 3 h culture, (b, e) fluorescent micrographs presenting F-actin in the cytoskeleton, (c, f) fluorescent micrographs of cell nuclei stained by DAPI, the scale bar is 100 μm.

The multiscale patterns of proteins have great potentials in the fields of biosensors, biointerfaces and research of cell behavior due to their advantages. For example, proteins present in 3D distributions on the polymer brush as a result of the 3D distributions of hydroxyl groups on the PHEMA brush. The protein patterns are held robustly in place by covalent bonds between the protein and the polymer brush. In addition, the polymer brush, which serves as the linkers between proteins and substrates, are long enough that they can prevent denaturation of proteins when they absorb on the substrate. Finally, complex, multiscale and gradient protein patterns can be prepared arbitrarily to any desired designs.

3.4. Cell Adhesion on the Multiscale Patterns of Proteins. The multiscale patterns of proteins are an ideal matrix to promote cell adhesion and to prepare cell patterns. FN patterns were used to perform experiments of cell culture. Cell experiments confirmed that mouse MC3T3-E1 osteblasts adhered well onto the multiscale patterns of FN resulting in organized cell patterns (Figure 5), and the cells maintained good biological activity (see Figure S7 in the Supporting Information). In our experiments, after being cultured for three days, we found that the cell patterns were maintained well. Figure 5a, d present that most of the cells adhere onto the FN regions, because the FN can promote cell adhesion. To explore the organization of actin filaments, we stained the F-actin in the cytoskeleton by tetramethylrhodamine B isothiocyanate (TRITC) labeled phallaoidin. The actin localizes in the region of FN in an organized fashion (Figure 5b, e). 4,6-diamidina-2-phenylindole (DAPI) was employed to stain cell nuclei, which are clearly visualized in Figure 5c and f. All the observations in these cell experiments confirm that cells can adhere and spread on multiscale patterns of FN. Moreover, localizing a single cell can be realized with the assistance of multiscale patterns with a diameter of 20 μm (Figure 5b, c). More importantly, taking advantage of microstripe patterns of FN, the adhesion and elongation of cells can be controlled simultaneously (Figure 5e, f). These multiscale patterns of proteins will pave a possible way to extensively study cell-biomaterial interactions that rely on multiscale material features that are just like those found in the microenvironment of the ECM.[53−57]

4. CONCLUSION

In summary, we have presented a method to prepare multiscale and gradient patterns of proteins. The proteins were immobilized on the PHEMA brush patterns by covalent bonds and maintained their biological activity. Making use of this technique, protein patterns with different architectures and feature sizes have been prepared and the size of sample can be up to 4 cm^2. In addition, as-prepared patterns of FN can promote cell adhesion and cell location. This technique for preparing protein patterns possesses several advantages, such as high-throughput, parallel fabrication and cost-efficiency. As a result, such patterns of proteins are very promising for extensive investigations in biomaterial and related areas.

■ ASSOCIATED CONTENT

Supporting Information

AFM images of PHEMA brush film with a height of 130 nm and the plot of PHEMA brush film thickness as a function of polymerization time; SEM images of 2D PS colloidal crystals with periods of 580 nm and 320 nm, respectively; AFM images of PHEMA brush nanopatterns with a period of 320 nm and with different height; the height of PHEMA nanodot, after conjugating DSC, and after conjugating IgG; 3D AFM images of human IgG; the fluorescent photograph of the multiscale and gradient IgG patterns after bonding FITC-anti-IgG; and the fluorescent micrograph of cells after viability staining by FDA. This material is available free of charge via the Internet at http://pubs.acs.org.

■ AUTHOR INFORMATION

Corresponding Author

*E-mail: byangchem@jlu.edu.cn. Fax: +86 431 85193423.

Notes

The authors declare no competing financial interest.

■ ACKNOWLEDGMENTS

This work was supported by the National Science Foundation of China (Grants 21222406, 91123031, 21074048, 20921003, 30830108) and the National Basic Research Program of China (2012CB933800).

■ REFERENCES

(1) Christman, K. L.; Enriquez-Rios, V. D.; Maynard, H. D. *Soft Matter* **2006**, *2*, 928−939.

(2) Jonkheijm, P.; Weinrich, D.; Schröder, H.; Niemeyer, C. M.; Waldmann, H. *Angew. Chem. Int. Ed.* **2008**, *47*, 9618−9647.

(3) Torres, A. J.; Wu, M.; Holowka, D.; Baird, B. *Annu. Rev. Biophys.* **2008**, *37*, 265−288.
(4) Schlapak, R.; Danzberger, J.; Haselgrübler, T.; Hinterdorfer, P.; Schüffler, F.; Howorka, S. *Nano Lett.* **2012**, *12*, 1983−1989.
(5) Taylor, Z. R.; Patel, K.; Spain, T. G.; Keay, J. C.; Jernigen, J. D.; Sanchez, E. S.; Grady, B. P.; Johnson, M. B.; Schmidtke, D. W. *Langmuir* **2009**, *25*, 10932−10938.
(6) Bettinger, C. J.; Langer, R.; Borenstein, J. T. *Angew. Chem., Int. Ed.* **2009**, *48*, 5406−5415.
(7) Kim, D. -H.; Lee, H.; Lee, Y. K.; Nam, J.-M.; Levchenko, A. *Adv. Mater.* **2010**, *22*, 4551−4566.
(8) Reyes, C. D.; Petrie, T. A.; Burns, K. L.; Schwartz, Z.; Garcia, A. J. *Biomaterials* **2007**, *28*, 3228−3235.
(9) Khademhosseini, A.; Langer, R.; Borenstein, J.; Vacanti, J. P. *Proc. Natl. Acad. Sci. U.S.A.* **2006**, *103*, 2480−2487.
(10) Whitesides, G. M.; Ostuni, E.; Takayama, S.; Jiang, X.; Ingber, D. E. *Annu. Rev. Biomed. Eng.* **2001**, *3*, 335−373.
(11) Berbard, A.; Renault, J. P.; Michel, B.; Bosshard, H. R.; Delamarche, E. *Adv. Mater.* **2000**, *12*, 1067−1070.
(12) Lee, K.-B.; Park, S.-J.; Mirkin, C. A.; Smith, J. C.; Mrksich, M. *Science* **2002**, *295*, 1702−1705.
(13) Wu, C.-C.; Reinhoudt, D. N.; Otto, C.; Subramaniam, V.; Velders, A. H. *Small* **2011**, *7*, 989−1002.
(14) Aydin, D.; Schwieder, M.; Louban, I.; Knoppe, S.; Ulmer, J.; Haas, T. L.; Walczak, H.; Spatz, J. P. *Small* **2009**, *5*, 1014−1018.
(15) Singh, G.; Pillai, S.; Arpanaei, A.; Kingshott, P. *Adv. Mater.* **2011**, *23*, 1519−1523.
(16) Gu, Z.; Huang, S.; Chen, Y. *Angew. Chem., Int. Ed.* **2009**, *48*, 952−955.
(17) Wang, C.; Zhang, Y. *Adv. Mater.* **2005**, *17*, 150−153.
(18) Maury, P.; Escalante, M.; Péter, M.; Reinhoudt, D. N.; Subramaniam, V.; Huskens, J. *Small* **2007**, *3*, 1584−1592.
(19) Malmström, J.; Christensen, B.; Jakobsen, H. P.; Lovmand, J.; Foldbjerg, R.; Sørensen, E. S.; Sutherland, D. S. *Nano Lett.* **2010**, *10*, 686−694.
(20) Feng, C. L.; Embrechts, A.; Bredebusch, I.; Schnekenburger, J.; Domschke, W.; Vancso, G. J.; Schönherr, H. *Adv. Mater.* **2007**, *19*, 286−290.
(21) Christman, K. L.; Schopf, E.; Broyer, R. M.; Li, R. C.; Chen, Y.; Maynard, H. D. *J. Am. Chem. Soc.* **2009**, *131*, 521−527.
(22) Lee, S. W.; Oh, B.-K.; Sanedrin, R. G.; Salaita, K.; Fujigaya, T.; Mirkin, C. A. *Adv. Mater.* **2006**, *18*, 1133−1136.
(23) Hoff, J. D.; Cheng, L.-J.; Meyhöfer, E.; Guo, L. J.; Hunt, A. J. *Nano Lett.* **2004**, *4*, 853−857.
(24) Ducker, R. E.; Janusz, S.; Sun, S.; Leggett, G. J. *J. Am. Chem. Soc.* **2007**, *129*, 14842−14843.
(25) Coyer, R.; Delamarche, E.; García, A. J. *Adv. Mater.* **2011**, *23*, 1550−1553.
(26) Haensch, C.; Hoeppener, S.; Schubert, U. S. *Chem. Soc. Rev.* **2010**, *39*, 2323−2334.
(27) Barbey, R.; Lavanant, L.; Paripovic, D.; Schüwer, N.; Sugnaux, C.; Tugulu, S.; Klok, H.-A. *Chem. Rev.* **2009**, *109*, 5437−5527.
(28) Dong, R.; Krishnan, S.; Baird, B. A.; Lindau, M.; Ober, C. K. *Biomacromolecules* **2007**, *8*, 3082−3092.
(29) Barbey, R.; Kauffmann, E.; Ehrat, M.; Klok, H.-A. *Biomacromolecules* **2010**, *11*, 3467−3479.
(30) Lin, X. K.; He, Q.; Li, J. B. *Chem. Soc. Rev.* **2012**, *41*, 3584−3593.
(31) Chen, T.; Amin, I.; Jordan, R. *Chem. Soc. Rev.* **2012**, *41*, 3280−3296.
(32) Ducker, R.; Garcia, A.; Zhang, J.; Chen, T.; Zauscher, S. *Soft Matter* **2008**, *4*, 1774−1786.
(33) Zhou, X. H.; Wang, X. L.; Shen, Y. D.; Xie, Z.; Zheng, Z. J. *Angew. Chem., Int. Ed.* **2011**, *50*, 6506−6510.
(34) Becer, C. R.; Haensch, C.; Hoeppener, S.; Schubert, U. S. *Small* **2007**, *3*, 220−225.
(35) Brinks, M. K.; Hirtz, M.; Chi, L. F.; Fuchs, H.; Studer, A. *Angew. Chem., Int. Ed.* **2007**, *46*, 5231−5233.
(36) Zhou, F.; Zheng, Z.; Yu, B.; Liu, W.; Huck, W. T. S. *J. Am. Chem. Soc.* **2006**, *128*, 16253−16258.
(37) Li, Y. F.; Zhang, J. H.; Fang, L. P.; Jiang, L. M.; Liu, W. D.; Wang, T. Q.; Cui, L. Y.; Sun, H. C.; Yang, B. *J. Mater. Chem.* **2012**, *22*, 25116−25122.
(38) He, Q.; Küller, A.; Grunze, M.; Li, J. B. *Langmuir* **2007**, *23*, 3981−3987.
(39) He, Q.; Kueller, A.; Schilp, S.; Leisten, F.; Kolb, H.-A.; Grunze, M.; Li, J. B. *Small* **2007**, *3*, 1860−1865.
(40) He, Q.; Tian, Y.; Küller, A.; Grunze, M.; Gölzhäuser, A.; Li, J. B. *J. Nanosci. Nanotechnol.* **2006**, *6*, 1838−1841.
(41) Benetti, E. M.; Acikgoz, C.; Sui, X.; Vratzov, B.; Hempenius, M. A.; Huskens, J.; Vancso, G. J. *Adv. Funct. Mater.* **2011**, *21*, 2088−2095.
(42) Li, Y. F.; Zhang, J. H.; Zhu, S. J.; Dong, H. P.; Jia, F.; Wang, Z. H.; Sun, Z. Q.; Zhang, L.; Li, Y.; Li, H. B.; Xu, W. Q.; Yang, B. *Adv. Mater.* **2009**, *21*, 4731−4734.
(43) Zhang, J. H.; Li, Y. F.; Zhang, X. M.; Yang, B. *Adv. Mater.* **2010**, *22*, 4249−4269.
(44) Yang, S.-M.; Jang, S. G.; Choi, D.-G.; Kim, S. H.; Yu, K. *Small* **2006**, *2*, 458−475.
(45) Li, Y. F.; Zhang, J. H.; Yang, B. *Nano Today* **2010**, *5*, 117−127.
(46) Li, Y. F.; Zhang, J. H.; Fang, L. P.; Wang, T. Q.; Zhu, S. J.; Li, Y.; Wang, Z. H.; Zhang, L.; Cui, L. Y.; Yang, B. *Small* **2011**, *7*, 2769−2774.
(47) Li, Y. F.; Zhang, J. H.; Zhu, S. J.; Dong, H. P.; Wang, Z. H.; Sun, Z. Q.; Guo, J. R.; Yang, B. *J. Mater. Chem.* **2009**, *19*, 1806−1810.
(48) Li, Y. F.; Zhang, J. H.; Wang, T. Q.; Zhu, S. J.; Yu, H. J.; Fang, L. P.; Wang, Z. H.; Cui, L. Y.; Yang, B. *J. Phys. Chem. C* **2010**, *114*, 19908−19912.
(49) Paik, M. Y.; Xu, Y.; Rastogi, Tanaka, A. M.; Yi, Y.; Ober, C. K. *Nano Lett.* **2010**, *10*, 3873−3879.
(50) Jeon, H.; Schmidt, R.; Barton, J. E.; Hwang, D. J.; Gamble, L. J.; Castner, D. G.; Grigoropoulos, C. P.; Healy, K. E. *J. Am. Chem. Soc.* **2011**, *133*, 6138−6141.
(51) Nie, Z. H.; Kumacheva, E. *Nat. Mater.* **2008**, *7*, 277−290.
(52) Campo, A. del; Arzt, E. *Chem. Rev.* **2008**, *108*, 911−945.
(53) Liu, P.; Sun, J.; Huang, J.; Peng, R.; Tian, J.; Ding, J. *Nanoscale* **2010**, *2*, 122−127.
(54) Hoover, D. K.; Chan, E. W. L.; Yousaf, M. N. *J. Am. Chem. Soc.* **2008**, *130*, 3280−3281.
(55) Stevens, M. M.; George, J. H. *Science* **2005**, *310*, 1135−1138.
(56) Zhang, J.-T.; Nie, J.; Mühlstädt, M.; Gallagher, H.; Pullig, O.; Jandt, K. D. *Adv. Funct. Mater.* **2011**, *21*, 4079−4087.
(57) Torres, A. J.; Wu, M.; Holowka, D.; Baird, B. *Annu. Rev. Biophys.* **2008**, *37*, 265−288.